# Genetic Algorithms for Distributed MIMO Radar Antenna Position Optimization


Salvatore Maresca
*IEIIT Institute*
*National Research Council (CNR)*
Pisa, Italy
salvatore.maresca@cnr.it

Antonio Malacarne
*PNTLab Institute*
*Nat. Interuniv. Cons. for Telecom. (CNIT)*
Pisa, Italy
antonio.malacarne@cnit.it

Malik Muhammad Haris Amir
*TeCIP Institute*
*Sant'Anna School of Advanced Studies (SSSA)*
Pisa, Italy
malikmuhammadharis.amir@santannapisa.it

Fawad Ahmad
*TeCIP Institute*
*SSSA*
Pisa, Italy
fawad.ahmad@santannapisa.it

Gaurav Pandey
*TeCIP Institute*
*SSSA*
Pisa, Italy
gaurav.pandey@santannapisa.it

Antonella Bogoni
*PNTLab Institute*
*CNIT*
Pisa, Italy
antonella.bogoni@cnit.it

Mirco Scaffardi
*PNTLab Institute*
*CNIT*
Pisa, Italy
mirco.scaffardi@cnit.it



***Abstract*—In multiple-input multiple-output (MIMO) radars, carrier frequency, signal bandwidth and antenna geometry have a deep impact on the ambiguity function (AF). In particular for systems employing widely separated antennas, sidelobes and azimuth ambiguities may appear in the MIMO-AF, potentially leading to a degradation of the system detection and localization capabilities.**

**The aim of this paper is to optimize antenna positions along the MIMO baseline using genetic algorithms (GAs). Key performance indicators (KPIs), such as the peak-to-maximum and peak-to-average sidelobe ratios, as well as the range and cross-range resolutions are investigated as potential optimization criteria.**

**As a practical study case, a MIMO radar working the in X-band is simulated. The system employs two transmitters (TXs) and four receivers (RXs), with free-located TX-RX antenna pairs. The analysis is conducted for a point-like target at different positions. The optimization is carried out by means of the GA-based function library available in MATLAB©, selecting both single and multiple KPIs as optimization criteria. In this latter case, the advantage is the optimization of more KPIs at the same time, however at the expense of a larger computation time.**



***Index Terms*—MIMO Radar, Ambiguity Function, Antenna Position Optimization, Genetic Algorithm, Key Performance Indicators.**


## I. Introduction

The ever increasing demand of systems with superior resolution, stability and accuracy in high-precision civilian and industrial applications [1], [2] is pushing radars to become even more ubiquitous sensors [3].

In this context, the ceaseless progress in the miniaturization of electronic components, and the advancements in microwave photonics (MWP) techniques [4]–[6], are accelerating the realization of coherent multiple-input multiple-output (MIMO) radars, which were theorized almost twenty years ago [7] and that can be categorized in systems with co-located antennas [8] and systems with widely separated antennas [9].

Focusing on this second type of architecture, several parameters influence the overall peak-to-sidelobe ratio (PSR) of the MIMO ambiguity function (AF). As pointed out in [9], not only increasing the spatial information brings a reduction of the sidelobe level, but also the fractional bandwidth of the signal (i.e., the bandwidth used in transmission with respect to the carrier frequency) and the antenna geometry have a deep impact on the overall PSR [10], [11].

Thus, the concept of *information diversity* was introduced in [12], with the aim of understanding the system effectiveness in detecting and resolving closely spaced targets, as well as in suppressing sidelobes in the MIMO-AF at the varying of system geometry and frequency parameters.

For this reason, performance metrics were proposed and evaluated to characterize the effects that information diversity has on MIMO radars with widely separated antennas [13]. Among these, the peak-to-maximum and peak-to-average sidelobe ratios, as well as the range and cross-range resolutions were proposed as performance metrics.

On the other hand, these KPIs could reveal precious also for optimizing the TX and RX antenna positions along the MIMO baseline. Generalizing the study conducted in [14], this paper attempts at outlining the most suitable criteria for optimizing the antenna positions using genetic algorithms (GAs).

Previous works on using GA-based techniques for antenna position optimization in sparse arrays and MIMO radars were presented in [15] and [16], respectively. However, in [16], dealing with co-located MIMO radars, and in [14], dealing with distributed MIMO radars, the optimization criterion consisted in the minimization of the peak sidelobe level (PSL).

In this paper, the analysis is conducted for a point-like


The project leading to this pubblication has received funding from Frontex under the Frontex Research Grants Programme. Call for Proposals 2022/CFP/RIU/01 - Grant Agreement No. 2023/350. This pubblication reflects only the authors' view. Neither the European Union nor Frontex are responsible for any use that may be made of the information it contains.

This work has also been partially funded by the EU under the Italian National Recovery and Resilience Plan (PNRR) of NextGenerationEU partnership on "Telecommunications of the Future" (PE00000001 - program "RESTART").

static target at different positions. The optimization is carried out by means of the GA-based function library available in MATLAB©, selecting both single and multiple KPIs as potential optimization criteria.

## II. Multiple-Input Multiple-Output Radars

A coherent MIMO radar can employ $M$ TX and $N$ RX radar front-ends, not necessarily co-located. The front-ends are denoted with $TX_m$ and $RX_n$, being $m = 1, \ldots, M$ and $n = 1, \ldots, N$, with $M \neq N$. For generality, $TX_m$ can operate at $L$ different radio frequencies (RFs).

### A. MIMO Signal Model

Let $s_m^{(l)}(t)$ be the low-pass equivalent of the signal transmitted by $TX_m$ at the $l$-th RF carrier, such that its waveform envelope has unit energy. The $M \times N$ antennas simultaneously illuminate $K$ scatterers $P_k$ having coordinates $(x_k, y_k)$, with $k = 1, \ldots, K$. These latter can belong to a single target or to multiple targets.

The time delay $\tau_{m,n}^{(k)}$ associated to the distance of $P_k$ with respect to $TX_m$ and $RX_n$ is evaluated as follows:

$$\tau_{m,n}^{(k)} = \frac{1}{c}\left[\mathbf{d}\left(TX_m, P_k\right) + \mathbf{d}\left(P_k, RX_n\right)\right], \tag{1}$$

where $c$ is the speed of light, and $\mathbf{d}\left(A, B\right)$ represents the Euclidean distance between the generic points $A \equiv (x_a, y_a)$ and $B \equiv (x_b, y_b)$ in the 2D space:

$$\mathbf{d}\left(A, B\right) = \sqrt{(x_a - x_b)^2 + (y_a - y_b)^2}. \tag{2}$$

In reception, the resulting $M \times N \times L$ individual *virtual channels* are separated for data processing. Thus, the low-pass equivalent of the signal received by $RX_n$ can be written as in [9]:

$$r_{m,n}^{(l)}(t) = \sum_{k=1}^{K} \zeta_{m,n}^{(k,l)} s_m^{(l)}\left[t - \tau_{m,n}^{(k)}\right] e^{j\varphi_{m,n}^{(l)}(t)} + w_{m,n}^{(l)}(t). \tag{3}$$

Here, $\zeta_{m,n}^{(k,l)}$ denotes the complex amplitude of the received signal contribution due to the $k$-th scatterer, whereas $\varphi_{m,n}^{(l)}(t)$ accounts for the overall phase shift of the virtual channel.

It is worth noticing that the analysis of such shifts is out of the scope of this work. However, a model of phase noise induced by RF signal distribution through optical fiber links was presented and its impact evaluated in [17]. Additional considerations about the total angular jitter introduced by the system architecture can be found in [18]. Moreover, phase terms due to Doppler shifts are to be considered yet.

In eq. (3), the term $w_n^{(l)}(t)$ represents the overall clutter-plus-noise contribution to the received signal, and, for simplicity, it is modelled as additive white Gaussian noise (AWGN) stochastic process. Finally, the terms $\zeta_{m,n}^{(k,l)}$ and $\tau_{m,n}^{(k)}$, with this latter described in eq. (1), depend on the bistatic geometry underlying the radar front-ends $TX_m$ and $RX_n$, and the scatterer $P_k$ over the $l$-th frequency channel $f_{RF}^{(l)}$:

$$\zeta_{m,n}^{(k,l)} = \frac{1}{D_{m,k}^{TX} D_{n,k}^{RX}} \sqrt{\frac{P_m^{(l)} G_m^{(l)} A_n^{(l)} \sigma_{m,n}^{(k,l)}}{(4\pi)^3 k_B B_n^{(l)} T_n^{(l)}}}, \tag{4}$$

where $D_{m,k}^{TX} = \mathbf{d}\left(TX_m, P_k\right)$ and $D_{n,k}^{RX} = \mathbf{d}\left(P_k, RX_n\right)$.

In eq. (4), $P_m^{(l)}$ and $G_m^{(l)}$ are respectively the transmitted power and antenna gain at $TX_m$ for the $l$-th waveform, $A_n^{(l)}$ is the effective area of the $RX_n$ antenna for the $l$-th RF carrier $f_{RF}^{(l)}$, $\sigma_{m,n}^{(k,l)}$ is the bistatic radar cross section (RCS) of scatterer $P_k$ observed by $TX_m$ and $RX_n$, $k_B$ is the Boltzmann's constant, $B_n^{(l)}$ is the noise bandwidth (BW), $T_n^{(l)}$ is the noise temperature at $RX_n$.

### B. MIMO Radar Ambiguity Function

Let $\mathbf{\Theta}_k$ be the $k$-th vector of parameters to be estimated. Under the assumption that scatterers do not interfere with each other, $\mathbf{\Theta}_k$, which for simplicity consists in the generic target position $(x_k, y_k)$ in the 2D space, can be the determined from the maximum likelihood (ML) estimate evaluated from all the $M \times N \times L$ available virtual channels. As described in [9], the ML estimate can be obtained in two ways via the MIMO-AF.

The first way of calculating the MIMO-AF is based on a *non-coherent MIMO processing* approach, involving only the amplitude of the received signals. Instead, the second way is based on a *coherent MIMO processing* approach, taking into account also the phase of the received signals:

$$\text{MIMO-AF}_c\left(\mathbf{\Theta}_k\right) \propto \left| \sum_{m=1}^{M} \sum_{n=1}^{N} \sum_{l=1}^{L} \varepsilon_{m,n}^{(k,l)} \cdot \Psi_{m,n}^{(k,l)}\left[t, \tau_{m,n}^{(k,l)}\right] \right|^2, \tag{5}$$

where:

$$\Psi_{m,n}^{(k,l)}\left[t, \tau_{m,n}^{(k,l)}\right] = \int_{-\infty}^{+\infty} r_{m,n}^{(k,l)}(t) s_m^{(l)*}\left[t - \tau_{m,n}^{(k,l)}\right] dt \tag{6}$$

represents the cross-correlation between $r_{m,n}^{(k,l)}(t)$ and $s_m^{(l)}(t)$. To obtain an overall picture of the monitored area, the MIMO-AF in eq. (5) is evaluated for each point $(x, y)$ in the observation space. Finally, the exponential term:

$$\varepsilon_{m,n}^{(k,l)} = e^{-j2\pi f_{RF}^{(l)} \tau_{m,n}^{(k,l)}} \tag{7}$$

depends on the $l$-th RF carrier and on the underlying bistatic geometry among $TX_m$, $RX_n$ and the scattering element $P_k$. After this phase compensation, the complex correlation contributions in eq. (6) can be summed together coherently, as described by eq. (5).

### C. Key Performance Indicators

In technical terms, KPIs are parameters that quantify the performance of a system. In this paper, the relevant KPIs proposed in [12], identified for evaluating the performance of a MIMO radar with widely separated antennas, act as the criteria used by the genetic algorithm for the optimization of the antenna positions.

The GA, that will be presented in Section III, exploits the following KPIs both in an individual or joint manner (i.e., trying maximize two KPIs at the same time):

- Peak-to-Maximum Sidelobe Ratio (PMSR),
- Peak-to-Average Sidelobe Ratio (PASR),
- Range resolution ($\Delta R$) of the mainlobe,
- Cross-range resolution ($\Delta XR$) of the mainlobe.

## III. Genetic Algorithms for Antenna Position Optimization

In MIMO radars, the TX and RX antennas create a $M \times N$ equivalent virtual array given by the Kronecker product of the $M$-ary TX array with the $N$-ary RX array [19]. This way, it is like if the RX array were repeated for every transmitting antenna. However, this can lead to redundancy in the virtual array elements placement [20]. Therefore, it is necessary a robust procedure for optimizing the distribution of the MIMO radar antennas along the baseline.

Genetic algorithms represent a class of algorithms for solving both constrained and unconstrained optimization problems [21]–[23]. They follow an approach similar to the one driving biological evolution and natural selection. They can be applied to solve optimization problems in which the objective function is discontinuous, non-differentiable, stochastic, or highly nonlinear. Finally, they help optimizing the attributes of a given set of objects called *population*. The high-level flow diagram of the system optimization procedure based on genetic algorithm is sketched in Fig. 1, whereas the main differences with the statistical-based approach are summarized in Table I.

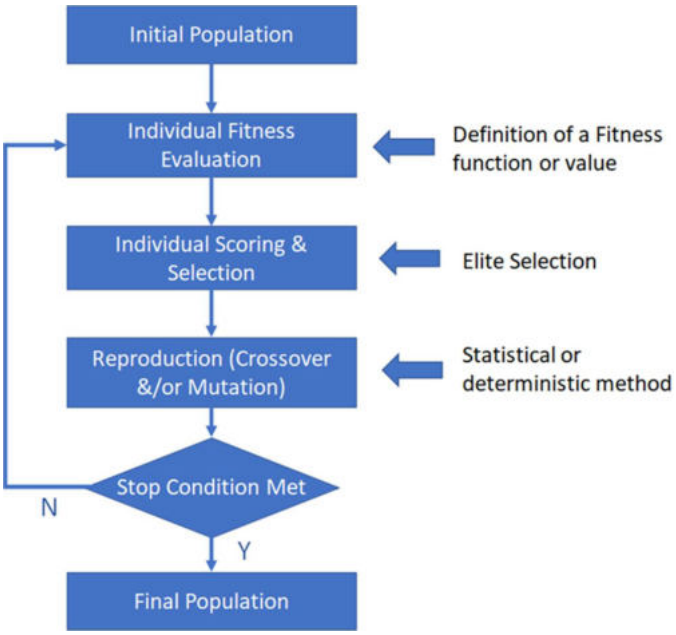


Fig. 1. High-level flow diagram of optimization based on genetic algorithm.

The core of the algorithm is the *fitness function*. In principle, the fitness function can be any of the already defined KPIs. Population reproduction can be obtained by mutations, i.e., statistical perturbations of the peripherals number and position. From a detection and estimation perspective, the main interest is in minimizing the sidelobes, understanding how they behave changing antennas disposition and number. Instead, from a target localization perspective, the aim is to minimize the system resolution, both in range and cross-range domains.

Since Matlab already has a set of functions related to genetic algorithms [24], this operation is performed using the `ga` and `gamultiobj` built-in functions. The first is used when the fitness function is represented by only one optimization criterion, whereas the second is used when multiple optimization criteria are used.

| Statistical Approach | Genetic Approach |
|---|---|
| The algorithm generates a single point at each iteration. The sequence of points approaches an optimal solution. | Generates a population of points at each iteration. The best point in in the population approaches an optimal solution. |
| Selects the next point in the sequence by a deterministic computation. | Selects the next population by computation which uses random number generators. |
| Typically converges quickly to a local solution. | Typically takes many function evaluations to converge. May or may not converge to a local or global minimum. |

TABLE I
Statistical vs Genetic Approach

## IV. Simulation Results

In the simulations, which replicate the in-door experimental scenario described in [25], the following setup parameters are considered for the coherent MIMO radar system:

- $M = 2$ TXs and $N = 4$ RXs over a 3 m baseline;
- Target distance from the baseline center equal to 3 and 30 m, for sudy case A and B, respectively;
- Frequency $f_{RF} = 10$ GHz, with signal bandwidth $B = 1$ GHz (i.e., $1/10$ fractional bandwidth).

The optimization procedure is carried out fixing one TX and one RX at the two extremes of the baseline. This allows to exploit the whole baseline extent and, thus, to achieve the maximum nominal azimuth resolution imposed by the baseline length given the RF frequency.

Seven criteria are considered as fitness functions for the GA. Four of them consist in optimizing separately PMSR, PASR, $\Delta R$ and $\Delta XR$. They are indicated with criteria no. 1, 2, 4 and 5, respectively. Instead, the last three criteria consist in the joint optimization of two KPIs simultaneously: PMSR and PASR, $\Delta R$ and $\Delta XR$, PMSR and $\Delta XR$ are indicated with criteria no. 3, 6 and 7, respectively.

### A. Analysis of Study Case A

The MIMO-AFs corresponding to the seven optimized antenna configurations are depicted in Fig. 2, 3 and 4. In particular, in Fig. 2 results of the optimization of PMSR, PASR and joint PMSR and PASR are shown. In Fig. 3, results of the optimization of $\Delta R$, $\Delta XR$ and joint $\Delta R$ and $\Delta XR$ are shown. Finally, in Fig. 4, results of the joint optimization of PMSR and $\Delta XR$ are shown. For completeness, the KPIs measured on the seven optimized MIMO configurations are summarized in Table II.

In general, regardless of the optimization criteria, the second TX is placed at the opposite side of the baseline with respect to the first one. Conversely, the RXs are more distributed along the baseline, especially when the optimization is done to reduce the MIMO-AF sidelobes (i.e., PMSR, PASR). In this

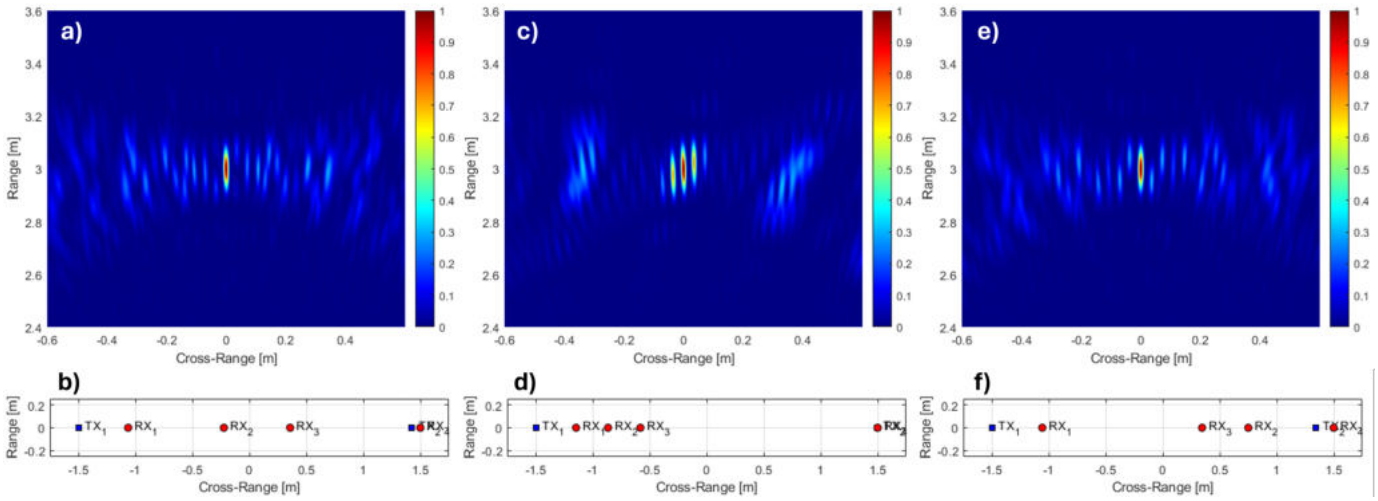


Fig. 2. MIMO baseline optimization based on the maximization of the peak-to-sidelobe ratios. No. 1) maximization of PMSR (left column): a) resulting coherent MIMO output, b) optimized MIMO baseline; No. 2) maximization of PASR (center column): c) resulting coherent MIMO output, d) optimized MIMO baseline; No. 3) joint maximization of PMSR and PASR (right column): e) resulting coherent MIMO output, f) optimized MIMO baseline.

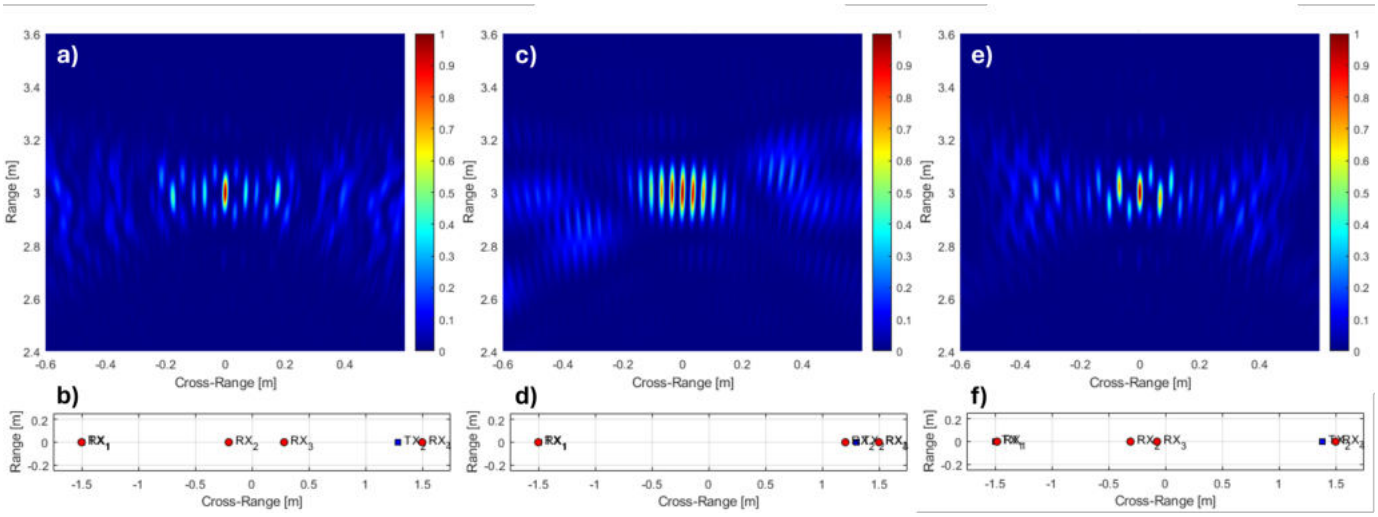


Fig. 3. MIMO baseline optimization based on the minimization of system resolution parameters. No. 4) minimization of $\Delta R$ (left column): a) resulting coherent MIMO output, b) optimized MIMO baseline; No. 5) minimization of $\Delta XR$ (center column): c) resulting coherent MIMO output, d) optimized MIMO baseline; No. 6) joint minimization of $\Delta R$ and $\Delta XR$ (right column): e) resulting coherent MIMO output, f) optimized MIMO baseline.

case, the maximization of PMSR is more effective than the maximization of PASR.

Instead, minimization of $\Delta R$ and/or $\Delta XR$ could result dangerous if they are the only optimization criteria, because the resulting sidelobe level may become too large. Thus, if minimization of resolution is sought, it should be always accompanied by minimization of sidelobes, too (see optimization criterion no. 7). Moreover, joint criteria have the advantage of optimizing more KPIs at the same time, even if at the expense of a larger computation time.

| No. | Opt. Criterion | PMSR [dB] | PASR [dB] | $\Delta R$ [m] | $\Delta XR$ [m] |
|---|---|---|---|---|---|
| 1) | PMSR | 5.3080 | 15.2199 | 0.1140 | 0.0150 |
| 2) | PASR | 1.3556 | 16.2447 | 0.1320 | 0.0135 |
| 3) | PMSR & PASR | 5.3042 | 15.4150 | 0.1260 | 0.0150 |
| 4) | $\Delta R$ | 2.9923 | 14.8281 | 0.1020 | 0.0150 |
| 5) | $\Delta XR$ | 0.2862 | 13.7568 | 0.1500 | 0.0135 |
| 6) | $\Delta R$ & $\Delta XR$ | 1.3683 | 14.9017 | 0.01020 | 0.0135 |
| 7) | PMSR & $\Delta R$ | 5.3144 | 15.0889 | 0.01260 | 0.0135 |

TABLE II
PERFORMANCE RESULTS OF THE OPTIMIZATION CRITERIA FOR A TARGET AT 3 M (STUDY CASE A)

### *B. Analysis of Study Case B*

For conciseness, the resulting MIMO-AFs and corresponding array configurations are not shown. However, the analysis of KPIs after antenna position optimization when the target is at 30 m from the centre of the MIMO baseline are summarized in Table III. When the target position changes in the space, results demonstrate that similar conclusions can be drawn

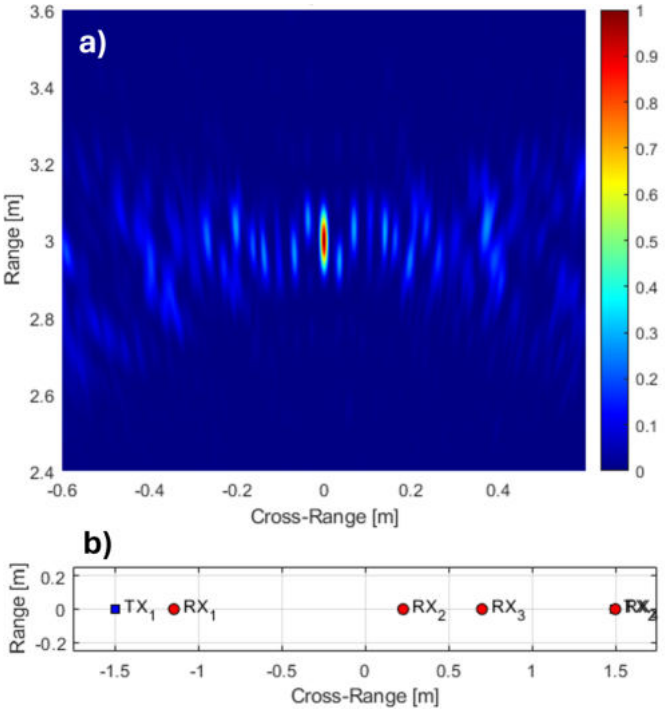


Fig. 4. MIMO baseline optimization based on criterion No. 7) joint maximization of PMSR and $\Delta XR$: a) resulting coherent MIMO output, b) optimized MIMO baseline.

| No. | Opt. Criterion | PMSR [dB] | PASR [dB] | $\Delta R$ [m] | $\Delta XR$ [m] |
|---|---|---|---|---|---|
| 1) | PMSR | 13.1291 | 21.4410 | 0.1380 | 0.1320 |
| 2) | PASR | 13.1029 | 23.0628 | 0.1380 | 0.1500 |
| 3) | PMSR & PASR | 13.1293 | 22.4838 | 0.1380 | 0.1410 |
| 4) | $\Delta R$ | 11.8667 | 20.1933 | 0.1380 | 0.1500 |
| 5) | $\Delta XR$ | 0.3600 | 10.1010 | 0.1380 | 0.1155 |
| 6) | $\Delta R$ & $\Delta XR$ | 1.0931 | 12.7024 | 0.1380 | 0.1150 |
| 7) | PMSR & $\Delta XR$ | 13.0308 | 21.2694 | 0.1380 | 0.1305 |

TABLE III
PERFORMANCE RESULTS OF THE OPTIMIZATION CRITERIA FOR A TARGET AT 30 M (STUDY CASE B)

on the effectiveness of KPIs to be chosen. Even if only two points in the monitored space have been considered, it is possible to conclude that every target position leads to a different optimized MIMO radar configuration. Thus, the optimum MIMO radar configuration should be retrieved by *averaging* the results over the whole area.

An additional prosecution of this work will concern the analysis of non-static targets, which entail phase compensation due to target-sensor relative velocity, as well as the optimization of MIMO radar baselines in close-to-reality scenarios (e.g., coastal-based systems, swarms of drones). Finally, due to the randomness in the optimization process, Monte Carlo simulations will be considered for obtaining a more accurate performance analysis of the algorithm. The aforementioned issues are currently object of ongoing research.

## V. CONCLUSION

In this paper, the optimization of antenna positions in a multiple-input multiple-output (MIMO) radar using genetic algorithms (GAs) has been presented. Key performance indicators (KPIs) measured on the MIMO ambiguity function, such as the peak-to-maximum and peak-to-average sidelobe ratios, respectively PMSR and PASR, as well as the range and cross-range resolutions have been investigated as potential optimization criteria. The optimization has been carried out by means of the GA-based function library available in MATLAB©, selecting both single and multiple KPIs as optimization criteria.

The maximization of PMSR is more effective than the maximization of PASR. Minimization of range and/or cross-range resolutions could result dangerous if they are the only optimization criteria. Thus, if minimization of resolution is sought, it should be always accompanied by minimization of sidelobes. Even if only two points in the monitored space have been considered, it is possible to conclude that every target position leads to a different optimized MIMO radar configuration. Thus, the optimum MIMO radar configuration could be retrieved by averaging the results over the whole area.

Additional prosecution of this work will concern the analysis of non-static targets, as well as the optimization of MIMO radar baselines in close-to-reality scenarios (e.g., coastal-based systems, swarms of drones). Finally, Monte Carlo simulations will be considered for obtaining a more accurate performance analysis of the algorithm, thus overcoming the solution randomness issue in the GA-based optimization process.

## REFERENCES

[1] M. S. Greco, J. Li, T. Long and A. Zoubir, "Advances in radar systems for modern civilian and commercial applications," *IEEE Sig. Proc. Mag.*, vol. 36, no. 4, pp. 13-15, Jul. 2019.
[2] M. S. Greco, J. Li, T. Long and A. Zoubir, "Advances in radar systems for modern civilian and commercial applications," *IEEE Sig. Proc. Mag.*, vol. 36, no. 5, pp. 16-18, Sep. 2019.
[3] J. J. Alter, *et al.*, "Ubiquitous radar: An implementation concept," *Proc. IEEE Radar Conf.*, pp. 65-70, 2004.
[4] J. Capmany, D. Novak, "Microwave photonics combines two worlds", *Nature Photonics*, vol. 1, pp. 319-330, 2007.
[5] J. McKinney, "Photonics illuminates the future of radar", *Nature*, vol. 507, pp. 310-312, 2014.
[6] G. Serafino, *et al.*, "Microwave Photonics for Remote Sensing: From Basic Concepts to High-Level Functionalities", *IEEE J. of Light. Tech.*, vol. 38, no. 19, pp. 5339-5355, 2020.
[7] E. Fishler, *et al.*, "MIMO radar: An idea whose time has come," *IEEE Radar Conf.*, pp. 71–78, 2004.
[8] J. Li, P. Stoica, "MIMO Radar with Colocated Antennas," *IEEE Sig. Proc. Mag.*, vol. 24, no. 5, pp. 106-114, Sept. 2007.
[9] A. M. Haimovich, *et al.*, "MIMO Radar with Widely Separated Antennas," *IEEE Sig. Proc. Mag.*, vol. 25, no. 1, pp. 116-129, 2008.
[10] B. Steinberg, "Radar Imaging from a Distorted Array: The Radio Camera Algorithm and Experiments", *IEEE Trans. on Antenna Prop.*, Vol. a-29, No. 5, Sep 1981.
[11] B. Steinberg, "Sidelobe Reduction of Random Arrays by Element Position and Frequency Diversity", *IEEE Trans. on Antenna Prop.*, Vol. a-31, No. 6, Nov 1983.
[12] S. Maresca, A. Malacarne, P. Ghelfi, and A. Bogoni, "Information Diversity in Coherent MIMO Radars," *2021 IEEE Radar Conference (RadarConf21)*, Atlanta, GA, USA, 2021, pp. 1-6.
[13] G. Serafino, *et al.*, "Key Performance Indicators for System Analysis of MIMO Radars with Widely Separated Antennas," *2022 19th European Radar Conference (EuRAD)*, Milan, Italy, 2022.

[14] L. Lembo, *et al.*, "Antenna Position Optimization in a MIMO Distributed Radar Network through Genetic Algorithms," *2019 20th International Radar Symposium (IRS)*, Ulm, Germany, 2019, pp. 1-6.
[15] L. Wang, and D. Fang, "Using GA to Synthesize Sparse Array", *Electrical Science Journal*, vol. 31, no. 12, pp. 2135-2138, 2003.
[16] Z. Zhang, Y. Zhao, and J. Huang, "Array Optimization for MIMO Radar by Genetic Algorithms," *2009 2nd International Congress on Image and Signal Processing*, Tianjin, China, 2009, pp. 1-4.
[17] A. Malacarne, *et al.*, "Robustness of Photonics-based Coherent Multi-Band MIMO Radar to Fiber-based Signal Distribution," *2023 20th European Radar Conf. (EuRAD)*, Berlin, Germany, 2023, pp. 514-517.
[18] A. Bogoni, P. Ghelfi and F. Laghezza, Photonics for Radar Networks and Electronic Warfare Systems, London:IET SciTech Pub., 2019.
[19] J. He, *et al.*, "Optimizing thinned antenna array geometry in MIMO radar systems using multiple genetic algorithm," *2011 IEEE CIE International Conference on Radar*, Chengdu, China, 2011, pp. 971-974.
[20] J. Li, *et al.*, "On Parameter Identifiability of MIMO Radar", *IEEE Signal Processing Letters*, Vol. 14, No. 12, Dec 2007.
[21] Goldberg, David E., Genetic Algorithms in Search, Optimization & Machine Learning, Addison-Wesley, 1989.
[22] A. R. Conn, *et al.*, "A Globally Convergent Augmented Lagrangian Algorithm for Optimization with General Constraints and Simple Bounds", *SIAM Journal on Numerical Analysis*, vol. 28, no. 2, pp. 545–572, 1991.
[23] A. R. Conn, *et al.*, "A Globally Convergent Augmented Lagrangian Barrier Algorithm for Optimization with General Inequality Constraints and Simple Bounds", *Mathematics of Computation*, vol. 66, no. 217, pp. 261–288, 1997.
[24] https://it.mathworks.com/help/gads/genetic-algorithm.html
[25] A. Malacarne, *et al.*, "Coherent Dual-Band Radar-Over-Fiber Network With VCSEL-Based Signal Distribution," *IEEE J. Light. Technol.*, vol. 38, no. 22, pp. 6257-6264, 2020.